

A parametric study of implantation-induced variations on the mechanical properties of epitaxial GaN

This article has been downloaded from IOPscience. Please scroll down to see the full text article.

2002 J. Phys.: Condens. Matter 14 12953

(<http://iopscience.iop.org/0953-8984/14/48/337>)

View [the table of contents for this issue](#), or go to the [journal homepage](#) for more

Download details:

IP Address: 171.66.16.97

The article was downloaded on 18/05/2010 at 19:14

Please note that [terms and conditions apply](#).

A parametric study of implantation-induced variations on the mechanical properties of epitaxial GaN

P Kavouras, M Katsikini, Th Kehagias, E C Paloura, Ph Komninou¹,
J Antonopoulos and Th Karakostas

Department of Physics, Aristotle University of Thessaloniki, 54124 Thessaloniki, Greece

E-mail: komnhnoy@auth.gr

Received 27 September 2002

Published 22 November 2002

Online at stacks.iop.org/JPhysCM/14/12953

Abstract

Doping of GaN through ion implantation permits improved control of the dopant profile and dose, while it also modifies the film's mechanical properties such as microhardness. We discuss the effect of Si⁺- and Mg⁺-ion implantation on the mechanical properties of GaN films grown by electron cyclotron resonance plasma-assisted molecular beam epitaxy on sapphire substrates. The changes of the mechanical properties are studied using the static indentation method and they are discussed in conjunction with results from near-edge x-ray absorption fine-structure spectroscopy. Transmission electron microscopy is used for the microstructural characterization of selected implanted specimens. The static indentation test method was applied utilizing Vickers and Knoop diamond indenters. The microhardness results are absolved from the influence of the substrate through the implementation of a well-established deconvolution method. The elastoplastic response of the films are compared and discussed on the basis of the proportional specimen resistance model and the form of the indentation size effect curves.

1. Introduction

High-dose ion implantation comprises an attractive method for several technological applications in the fabrication of GaN-based devices such as selective-area doping. However, it produces point and extended defects, while it can render GaN films amorphous. The implanted lattice damage constitutes the main cause of the present limitations of implantation as a means of selective-area doping, because *in situ* control of implantation damage has yet to be achieved. In addition to the lattice damage, implantation results in significant alteration of the mechanical properties of the implanted epilayer [1, 2]. Despite the fact that several studies have been made on the determination of mechanical properties of as-grown GaN films [3], implanted GaN has

¹ Author to whom any correspondence should be addressed.

Table 1. Sample names, implantation conditions and a summary of the mechanical property results. The energy of the implanted ions was 100 keV. The area under RLA was derived from the NEXAFS measurements.

Sample type	Implanted ion	Dose (cm ⁻²)	Area under peak A	H_K (GPa)	PSR model, α_1 parameter	P_c (N)
As-grown	—	—	—	13.7	0.0967	<4.0
GaN:Si14	Si ⁺	1×10^{14}	0.25	13.9	0.0961	3.3
GaN:Si16	Si ⁺	1×10^{16}	0.46	18.4	0.0913	2.5
GaN:Si18	Si ⁺	1×10^{18}	0.00	3.8	0.0899	2.3
GaN:Mg15	Mg ⁺	1×10^{15}	0.35	14.7	0.0903	1.7
GaN:Mg17	Mg ⁺	1×10^{17}	1.27	15.8	0.0843	1.8

received scant attention. Understanding the deformation behaviour of ion-beam-modified GaN films is not only important for contact damage issues in the GaN industry, but is also necessary for understanding the evolution of the structural characteristics of GaN under ion bombardment.

The mechanical properties of GaN films are usually studied by the conventional microhardness method or the continuous depth-sensing method (usually referred to as the nanohardness method). In the present work the conventional microhardness testing method is applied to monitor the alteration of mechanical properties induced by the implantation of Si and Mg ions in hexagonal GaN films epitaxially grown on (0001) sapphire. The above technique was selected because surface roughness, which is strongly affected by the implantation process, especially under conditions that favour severe damage and/or amorphization [4], does not pose a problem in microhardness measurements.

The mechanical properties of the implanted films are discussed in conjunction with the post-implantation microstructural characteristics of the implanted epilayers, obtained with near-edge x-ray absorption fine-structure (NEXAFS) spectroscopy and transmission electron microscopy (TEM). A NEXAFS spectrum maps the density of empty states and, as was recently demonstrated, its features depend on the film's symmetry (zinc-blende or wurtzite) [5]. In addition to that, NEXAFS spectroscopy can be used to monitor the implantation-induced damage, since the increase of the static disorder and the introduction of defect empty states modify the NEXAFS characteristics in a quantitative manner [5]. Finally, the microstructural characteristics of the implanted epilayer were determined with TEM observations.

2. Growth conditions and experimental details

The GaN sample, which was used for the implantation, was grown by electron cyclotron resonance molecular beam epitaxy (ECR-MBE) on a (0001) sapphire substrate, using a plasma source for the activation of nitrogen [6]. A buffer layer was grown at 500–600 °C on the nitrided [7] sapphire substrate and the GaN epilayer was deposited at 700 °C. The GaN sample was cut into several pieces that were implanted using Mg and Si ions to the doses and at the energies listed in table 1. The implanted ions reach a maximum depth of 200 nm [8].

A Knoop indenter (microhardness tester Anton Paar, MHT-10) was utilized for the microhardness measurements. The indentation size effect (ISE) curve was obtained in the load range of 0.1–0.8 N for all specimens presented in table 1. The upper limit was imposed from the requirement of avoiding production of surface microcracks and the lower in order to produce measurable indentation prints. Each microhardness value represents the mean value of 20 measurements. The ISE curves were used for the deconvolution of the microhardness

values of the implanted epilayer from that of the non-implanted portion of the film. The deconvolution method used in the present work is based on a weighted law of mixture that was originally developed by Jönsson and Hogmark [9]. In [9], the implanted epilayer was considered as the coating of the unimplanted portion of the film that was treated as the substrate [2]. The ISE curve of the unimplanted portion of the film was obtained from the as-grown GaN sample, which was used as a reference sample. The ISE curves were modelled on the basis of the proportional specimen resistance (PSR) model [10]. The susceptibility to microcrack formation was investigated utilizing the Vickers indenter geometry and the results were compared with the results from the PSR model.

The N-K-edge NEXAFS spectra were recorded at room temperature, using a monochromatized beam from the VLS-PGM monochromator at the electron storage ring BESSY-II in Berlin. An exit slit of 60 μm was used. The base pressure during the measurement was 1×10^{-7} Pa. The NEXAFS spectra were recorded at $\theta = 55^\circ$ (relatively to the sample surface), using a high-purity Ge fluorescence detector. The information depth of the fluorescence photons is 40 nm, i.e. the NEXAFS spectra probe only the implanted region.

The effect on the microstructure of the samples implanted with the highest Si dose was investigated using TEM methods. The specimens were prepared for cross-section observation using the standard procedure of mechanical thinning followed by ion-milling, at liquid nitrogen temperature. The TEM observations were carried out in a Jeol 120 CX electron microscope operated at 100 kV.

3. Results

3.1. Mechanical properties

The microhardness value of the as-grown specimen was measured to be 13.7 GPa; this value is in close agreement with previously published results [2, 11]. The deconvoluted microhardness values are summarized in table 1. The standard deviations in every case are between ± 0.25 and ± 0.35 GPa. Implantation with either Si or Mg with doses in the range 1×10^{15} – 1×10^{17} cm^{-2} leads to hardening of the GaN epilayer (table 1). The effect of Si-ion implantation on the microhardness value H_K is insignificant for an implant dose of 1×10^{14} cm^{-2} , while a severe decrease is observed for the dose 1×10^{18} cm^{-2} . The softening of the GaN:Si18 sample is attributed to amorphization of the epilayer, as identified by the NEXAFS and TEM characterization results (H_K decreases from 13.7 to 3.8 GPa). The ISE curves of all specimens were fitted by the application of the PSR model. The α_1 -parameter (table 1) represents the intensity of the ISE, and it decreases with increasing implantation dose, while it obtains higher values when Si is the projectile.

The minimum load for surface microcrack generation (P_c) of the as-grown reference sample is higher than the maximum load that can be exerted from the microhardness tester used in this work, which is 4.0 N. With increasing Si- and Mg-ion implantation dose, P_c decreases. In the case of Mg-ion implantation, P_c is lower.

3.2. NEXAFS characterization results

The N K-edge NEXAFS spectra of the samples under study are shown in figure 1. The spectrum of the as-grown sample shows a characteristic fine structure, which is the signature of hexagonal GaN [5]. Upon implantation with doses in the range 1×10^{14} – 1×10^{17} cm^{-2} , the NEXAFS spectra retain their main characteristics (number and energy positions of the resonances as well as their relative intensities). However, the implantation-induced static disorder causes

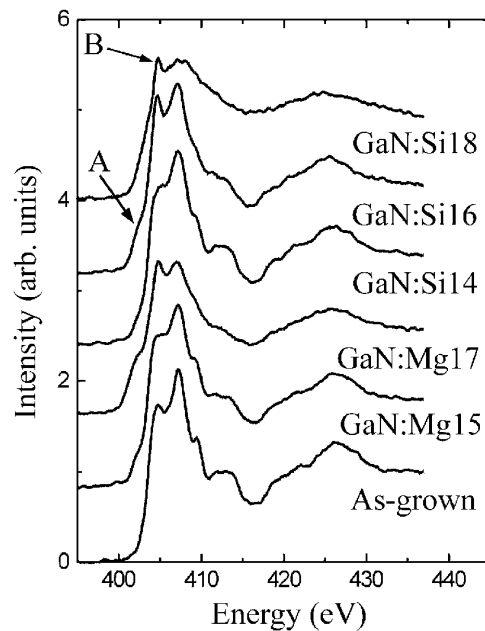


Figure 1. NEXAFS spectra of Mg- and Si-implanted GaN samples. The spectra are shifted along the y-axis for better comparison.

broadening of the NEXAFS peaks. When the dose exceeds the value of $1 \times 10^{17} \text{ cm}^{-2}$, the characteristic peaks are completely smoothed out, due to amorphization of the film. To explain this characteristic smoothing of the spectrum we have to consider that the absorption cross-section (σ) of an atom in a compound is a sum of different photoelectron scattering contributions [12]: (a) the single scattering of the first shell, (b) single scattering of the more distant shells and (c) the multiple scattering. As the static disorder due to the implantation increases, the single scattering from the first-nearest-neighbour shell (the tetrahedron around nitrogen) dominates the spectrum and the fine structure due to the (b) and (c) types of scattering is diminished. Therefore, it can be deduced that the GaN sample that was implanted with $1 \times 10^{18} \text{ cm}^{-2}$ Si became amorphous.

In addition to the broadening of the NEXAFS resonances, implantation introduces two defect-related resonance lines (RLs) denoted as A and B in the spectra of figure 1 (RLA and RLB, respectively). The characteristics of the resonances, i.e. energy position, FWHM and area under the peak, were determined after fitting the spectra, following a procedure described elsewhere [2]. RLA appears for all the implanted samples that retain their crystallinity (i.e. all the films except the one implanted with the dose $1 \times 10^{18} \text{ cm}^{-2}$); its intensity increases with the implantation dose and it is more prominent for the samples implanted with Mg. RLB has a very small full width at half-maximum (FWHM = 0.14 eV), it appears for implantation doses higher than $1 \times 10^{16} \text{ cm}^{-2}$ and its intensity increases with the dose. Due to its small FWHM, RLB can only be attributed to a defect that is localized on the absorbing atom and which is not affected by the intermediate- or long-range order of the sample.

Among the two RLs, RLA has been detected also for GaN samples implanted with N and O in the dose range 5×10^{13} – $5 \times 10^{14} \text{ cm}^{-2}$ and it has been assigned to nitrogen interstitials (N_i) [12]. According to theoretical calculations [13], N_i relaxes in the (100) split-interstitial configuration where the two N atoms occupy the same substitutional site and each one forms

two bonds with two Ga atoms. The two N atoms give π p-like antibonding mid-gap states, which can be detected by means of NEXAFS. Since the intensity of RLA increases with the implantation dose, it can be concluded that the concentration of the nitrogen interstitials also increases.

Unlike RLA, RLB appears at implantation doses higher than $1 \times 10^{16} \text{ cm}^{-2}$. A RL similar to RLB has been observed in ion-implanted Si_xN_y [14, 15] where its origin has been identified as the N dangling bond defect. According to theoretical calculations [16], significant amounts of threefold-coordinated N and Ga atoms exist in amorphous GaN. Although the implanted samples are not completely amorphous, some isolated amorphous nuclei are expected to occur [17] even at intermediate implantation doses. Therefore, it is proposed that RLB is assigned to the N dangling bond defect in GaN.

3.3. TEM observations

The cross-section transmission electron microscopy (XTEM) bright-field micrograph shown in figure 2(a) depicts the morphology of the GaN:Si18 sample near the surface of the film. A large amorphous area with an average width of 200 nm is detected at the top of the GaN epilayer. The black arrows denote the depth of the amorphization caused by the implanted Si ions. Furthermore, under the amorphous area that extends along the whole surface of the film, another heavily damaged band is observed (white arrows). This band, with an average width of 60 nm, although penetrated by the Si ions, has not become amorphous, as is verified from the dark-field (DF) image of figure 2(b). Figure 2(b), taken with the 0002 reflection of GaN, shows bright contrast for the damaged band as well as for the undamaged GaN, whereas the amorphous area is clearly not in contrast. This evidently indicates that the damaged band is still crystalline GaN. Thus, the corresponding amorphization produced by the ions at the GaN surface extends to a depth of 200 nm. The TEM observations confirm that the thickness of the implanted epilayer that was used for the deconvolution of its microhardness value is correct.

4. Discussion

The hardening effect, observed in the GaN:Si16, GaN:Mg15 and GaN:Mg17 samples, can be attributed to the increase of the concentration of the interstitial nitrogen ions in the implanted epilayer. The concentration of interstitial nitrogen atoms is expected to increase with the implantation dose, as was verified by the increase of the intensity of RLA in the NEXAFS measurements. In the present work this result is independent of the nature of the implanted ion. The hardening effect of the interstitial nitrogen ions is attributed to the increased flow stress due to dislocation anchoring on implanted ions and/or reduction of the available slip planes due to the increase of the static disorder; a similar behaviour was observed in nitrogen-ion implantation [2]. The above arguments are supported by the observation that the main deformation mechanism of wurtzite GaN films grown on sapphire substrates appears to be dislocation plasticity [18], specifically the nucleation of slip on the basal planes, with dislocations being nucleated on additional planes on further loading. Consequently, the fact that GaN:Si14 does not exhibit any measurable hardening is consistent with the above analysis, since the structure of the implanted epilayer is roughly the same as that of the as-grown one.

Implantation with a dose of $1 \times 10^{18} \text{ cm}^{-2}$ resulted to the amorphization of a surface layer that was detected by means of NEXAFS and TEM. The amorphized epilayer extends 200 nm below the film surface, as resolved by TEM observations. However, the amorphous layer is followed by a heavily damaged, 60 nm thick band. The amorphized epilayer exhibits a striking decrease in the microhardness value: it decreases to 3.8 GPa. A comparable

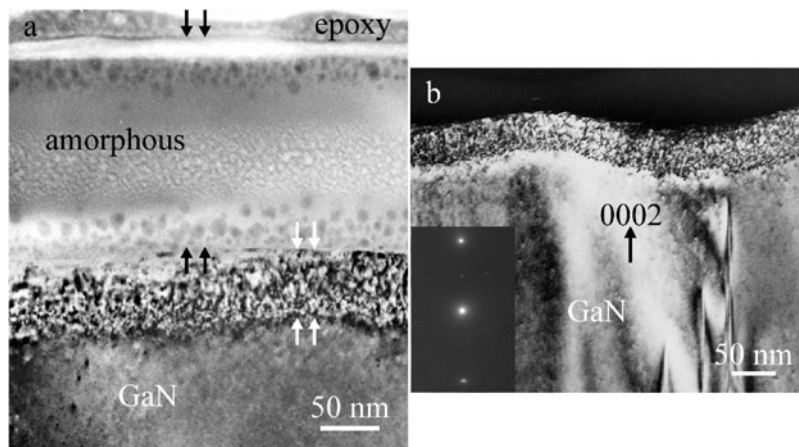


Figure 2. (a) A bright-field XTEM micrograph with the $000\bar{2}$ reflection illustrating the area of the epilayer that is amorphized by the implantation of Si ions (black arrows), as well as the damaged band (white arrows). (b) A DF image with the 0002 reflection of GaN revealing the crystallinity of the damaged band. The corresponding diffraction pattern is given as an inset.

microhardness value decrease has been reported for amorphized GaN with implantation of Au ions ($H_K = 2.4$ GPa) by Kucheyev *et al* [19]. The small difference in the microhardness values can be attributed to the different effect of the defect band due to implantation (figure 2(b)), which was observed to be thinner in the previously mentioned work. Although analogous hardening effects were observed for Si- and Mg-ion implantation, the microhardness value increase is not quantitatively comparable. That is, despite the fact that the interstitial nitrogen concentration in GaN:Mg17 is higher than that in GaN:Si16 (table 1), the latter is harder.

Surface microcrack formation in the implanted films initiates at lower loads than for the as-grown film (table 1). Consequently, the efficiency of fracture in acting as an indentation energy absorption mechanism increases with increasing implantation dose. This may rely on the fact that surface energy is decreased as a result of the adsorption of the implanted species at the crack tip [20]. This behaviour can be connected with the reduced role of dislocation plasticity in the higher-dose regions; i.e. fracture acts as a stress-relief mechanism partially substituting dislocation plasticity. Additionally, the intensity of the ISE gradually decreases with increasing implantation dose. According to the PSR model, the ISE is produced from two main contributions: (a) from the elastic resistance of the test specimen and (b) from the frictional effects at the indenter facet/specimen interface. It can thus be deduced that the elastic resistance of the implanted epilayers (or the elastic recovery) is reduced, since alteration of the frictional effects is not significant. Reduction of the ISE has been only reported for surfaces coated with a lubricant [21]. This reduced elastic resistance could be an additional possible explanation of the reduced value of P_c : a lower proportion of the indentation load can be relieved by elastic recovery and as a result fracture initiates more easily.

5. Conclusions

Significant hardening of GaN epilayers is produced through Si-ion implantation with doses of $1 \times 10^{16} \text{ cm}^{-2}$, while at a dose of $1 \times 10^{14} \text{ cm}^{-2}$ no measurable hardening is observed. The hardening effect can be attributed to the fact that dislocation movement is more difficult in the damaged implanted epilayer, due to (a) dislocation anchoring on interstitial atoms and/or

(b) reduction in the number of available slip planes. However, for implantation dose of $1 \times 10^{18} \text{ cm}^{-2}$, surface amorphization takes place and a noticeable softening occurs. Mg-ion implantation exhibits a similar hardening behaviour, for implantation doses of 1×10^{15} and $1 \times 10^{17} \text{ cm}^{-2}$. Nevertheless, Mg-ion implantation produces a higher concentration of nitrogen interstitials and an apparently lower hardening effect. For both implanted species, the minimum load for surface fracture decreases with increasing implantation dose. This effect can be attributed to the decreased efficiency of dislocation plasticity and elastic recovery in acting as indentation absorption mechanisms for implantation doses $\geq 1 \times 10^{16} \text{ cm}^{-2}$.

Acknowledgments

This work was partially supported by the EU contract HPRN-CT-1999-00040. The experimental work at BESSY was realized with financial support from the EC-HPRI-1999-CT-00028 programme. As-grown films were kindly provided by Professor T D Moustakas, and implantation was performed by Dr A Markwitz. One of the authors (M Katsikini) acknowledges financial support from the Greek State Scholarship's Foundation.

References

- [1] Kucheyev S O, Bradby J E, Williams J S, Jagadish C, Swain M V and Li G 2001 *Appl. Phys. Lett.* **78** 156–8
- [2] Kavouras P, Katsikini M, Vouroutzis N, Lioutas C B, Paloura E C, Antonopoulos J and Karakostas Th 2001 *J. Cryst. Growth* **230** 454–8
- [3] Kucheyev S O, Williams J S and Pearton S J 2001 *Mater. Sci. Eng. R* **33** 51–107
- [4] Vouroutzis N 2002 private communication
- [5] Katsikini M, Paloura E C and Moustakas T D 1998 *J. Appl. Phys.* **83** 1437
- [6] Moustakas T D and Molnar R J 1993 *Mater. Res. Soc. Symp. Proc.* **281** 753
- [7] Moustakas T D, Lei T and Molnar R J 1993 *Physica B* **185** 36
- [8] Zolper J C, Tan H H, Williams J S, Zou J, Cockayne D J H, Pearton S J, Hagerott C M and Karliceck R F Jr 1997 *Appl. Phys. Lett.* **70** 729
- [9] Jönsson B and Hogmark S 1984 *Thin Solid Films* **114** 257
- [10] Li H and Bradt R C 1993 *J. Mater. Sci.* **28** 917
- [11] Nikolaev V I, Shpeĭzman V V and Smirnov B I 2000 *Phys. Solid State* **42** 428
- [12] Bugaev L A, Solonenko H V, Dmitrienko A P and Flank A M 2002 *Phys. Rev. B* **65** 24105
- [13] Neugebauer J and van de Walle C G 1994 *Phys. Rev. B* **50** 8067
- [14] Paloura E C, Knop A, Holldack K, Döbler U and Logothetidis S 1993 *J. Appl. Phys.* **73** 2995
- [15] Paloura E C 1997 *Appl. Phys. Lett.* **71** 3209
- [16] Stumm P and Drabold D A 1997 *Phys. Rev. Lett.* **79** 677
- [17] Liu C, Mensching B, Zeitler M, Volz K and Rauschenbach B 1998 *Phys. Rev. B* **57** 2530
- [18] Bradby J E, Kucheyev S O, Williams J S, Wong-Leung J, Swain M V, Munroe P, Li G and Phillips M R 2002 *Appl. Phys. Lett.* **80** 383
- [19] Kucheyev S O, Williams J S, Zou J, Bradby J E, Jagadish C and Li G 2001 *Phys. Rev. B* **63** 113202
- [20] Courtney T H (ed) 1990 *Mechanical Behaviour of Materials* (New York: McGraw-Hill)
- [21] Li H, Ghosh A, Han Y H and Bradt R C 1993 *J. Mater. Res.* **8** 1028